Parasitology Research (2025) 124:52
https://doi.org/10.1007/s00436-025-08480-6

RESEARCH

Functional annotation and analysis of the hard tick *Dermacentor nuttalli* midgut genes

Hejia Ma[1,3] · Lijun Jia[2] · Jian Feng[2] · Tianshuai Li[1] · Chao Li[1] · Jixu Li[1,3,4] · Xuenan Xuan[5] · Yali Sun[1,3,4]

Received: 12 August 2024 / Accepted: 5 March 2025

Abstract

Ticks are hematophagous vectors that transmit a variety of pathogens, posing significant threats to the health of both humans and animals. Tick midgut proteins play essential roles in blood digestion, feeding, toxic waste processing, and pathogen transmission. *Dermacentor nuttalli* is the primary vector of tick-borne pathogens, including rickettsioses in the Qinghai-Tibet Plateau. However, there is a lack of genomic, transcriptomic, and proteomic information regarding the biology of *D. nuttalli*. In this study, we assembled and compared the midgut transcriptomes of female *D. nuttalli* ticks at 0, 24, 48, 72, and 96 h during blood feeding, identifying the genes with differentially regulated expression following feeding. The obtained data were compiled and annotated in multiple databases including Nr, NT, PFAM, KOG, KEGG, and GO. The high-quality clean readings of midgut tissue at the different blood-feeding times were recorded as 22,524,912, 23,752,325, 20,377,718, 21,300,710, and 20,378,658, respectively. The transcripts were classified into eight large categories, including immunogenic proteases (8.37%), protease inhibitors (0.85%), transporters (3.96%), ligand binding proteins (1.98%), ribosomal function proteins (0.94%), heat shock proteins (0.30%), other proteases and miscellaneous proteins (57.61%), and unknown proteins (26.00%). Significant differences were observed in the genes obtained at 0, 24, 48, 72, and 96 h during blood feeding. The differentially expressed genes include catalytic proteins that play an important role in accelerating biochemical reactions, binding activity proteins which are involved in various molecular interactions, and proteins that actively participate in multiple metabolic pathways and cellular processes. Notably, the gene expression in the midgut of *D. nuttalli* shows dynamic changes every 24 h throughout the blood-feeding process. This change may represent an equivalent strategy of antigenic variation for ticks, designed to protect their essential feeding function against the host's immune system. The tick antigens identified in this study may serve as promising candidates for the development of effective vaccines or as drug targets for acaricides.

Keywords *Dermacentor nuttalli* · Midgut · RNA-seq · Blood feeding · Differential expression

Introduction

Ticks are hematophagous arthropods capable of transmitting a variety of pathogens, including viruses, bacteria, and protozoa (Zhao et al. 2021; Moraga-Fernández et al. 2023). This capability has made them a focal point in

Section Editor: Van Lun Low

Hejia Ma, Lijun Jia, and Jian Feng are co-first authors.

✉ Xuenan Xuan
gen@obihiro.ac.jp

✉ Yali Sun
yalisun@qhu.edu.cn

[1] College of Agriculture and Animal Husbandry, Qinghai University, Xining 810016, China

[2] Engineering Research Center of North-East Cold Region Beef Cattle Science & Technology Innovation, Ministry of Education, Yanbian University, Yanji 133002, China

[3] State Key Laboratory of Plateau Ecology and Agriculture, Qinghai University, Xining 810016, China

[4] Qinghai Provincial Key Laboratory of Pathogen Diagnosis for Animal Diseases and Green Technical Research for Prevention and Control, Qinghai University, Xining 810016, China

[5] National Research Center for Protozoan Diseases, Obihiro University of Agriculture and Veterinary Medicine, Obihiro, Hokkaido 0808555, Japan

Published online: 15 May 2025

public health policies. *Dermacentor nuttalli* is primarily distributed in northern China, Russia, North Korea, and Mongolia, where it is commonly found in arid grassland areas suitable for grazing cattle and sheep (Mediannikov et al. 2008). Notably, *D. nutalli* carries the pathogens such as *Anaplasma ovis*, *Rickettsia raoultii*, *Theileria luwenshuni*, *Brucella*, *Francisella tularensis*, and *Anaplasma phagocytophilum* (Wang et al. 2021; Shi et al. 2018). The presence of *D. nuttalli* and the pathogens it harbors has led to economic losses in the livestock industry and poses a threat to the health of the local population (Jongejan and Uilenberg 2004; Zhang et al. 2019).

In the absence of an effective anti-tick vaccine, the use of acaricides remains the most common approach for tick control (van Zyl et al. 2014). However, chemical acaricides are accompanied by serious environmental pollution and food source pollution (Webster et al. 2015). Therefore, vaccination is still advocated as a sustainable and environmentally friendly method for tick control (Mulenga et al. 2009). We are highly interested in understanding the tick feeding process. Consequently, transcriptome sequencing was carried out on ticks at different blood-feeding times. Our focus has been directed toward determining whether these physiologically important proteins can serve as critical targets for anti-tick vaccines.

Ticks have different developmental stages, and the feeding time varies in each stage. Different ticks have different generational cycles. The life cycle of *D. nuttalli* in laboratory-rearing showed that the average period of female adult engorgement was 11.4 days (Ma et al. 2023a, b). Before blood feeding, *D. nutalli* firmly attach themselves to the host's body. They cut through the host's epidermis with their chelicerae and then insert their mouthparts into the host's dermis (Šimo et al. 2017). Consequently, the small blood vessels and capillaries of the host may be significantly damaged leading to the formation of a blood pool and hemorrhagic damage in the host (Aounallah et al. 2020). There are three feeding stages in the blood-feeding process of a tick: the initial stage, during which the host is bitten; the prolonged slow-feeding stage, which lasts several days; and the rapid feeding stage, which occurs within approximately 1 day as the tick obtains a blood meal before completing the feeding process (Tirloni et al. 2020; Jmel et al. 2021). Once the tick ingests blood-containing pathogens, its midgut initiates a series of processes. It begins to digest the blood, process the toxic waste generated during digestion, and create a suitable environment for the potential proliferation of pathogens. Therefore, the tick midgut serves as the primary barrier for blood digestion and the entry of tick-borne pathogens (Kocan et al. 2004). To comprehend the physiological processes involved in blood feeding in ticks, it is essential to systematically investigate the contributing factors. This understanding aims to target the interactions among the tick, the animal host, and the tick-borne pathogens.

With the advent of next-generation sequencing technologies, the transcriptomes of tick midgut have been characterized (Anderson et al. 2008; Schwarz et al. 2014). Midgut transcriptomic analyses of different tick species have been reported, including *Ixodes ricinus* (Perner et al. 2016), *Haemaphysalis flava* (Xu et al. 2015), and *Amblyomma americanum* (Lu et al. 2024). The midgut of ticks begins to become active during the early stages of blood feeding. Bendele et al. and Lu et al investigated a range of physiological and immune responses that occur among ticks and hosts shortly after blood feeding begins. These responses include the host's immune defense mechanisms and the ticks' immune evasion strategies (Bendele et al. 2019; Lu et al. 2023). Overall, it is highly significant to investigate the potential mechanisms involved in the early stages of tick blood feeding.

Here, we report the results of the *D. nuttalli* midgut transcriptome analysis conducted at 0, 24, 48, 72, and 96 h during blood feeding. We analyzed the differentially expressed genes involved in the blood feeding of *D. nuttalli.* Additionally, we explored significant molecules associated with the midgut during tick feeding, which may serve as effective and environmentally friendly antigens for the development of drugs and vaccines aimed at controlling ticks populations (Nathaly Wieser et al. 2019; Šimo et al. 2017; Antunes et al. 2014; de la Fuente 2012).

Materials and methods

Ticks and laboratory animals

Dermacentor nuttalli specimens were collected in Haidong, Qinghai Province, China (102°09′–102°47′ E and 36°16′–36°40′ N) from March to April 2021. The *D. nutalli* adult ticks used in the study were from the second generation raised under laboratory conditions. The species of ticks was confirmed using morphological and molecular analysis. *D. nuttalli* ticks were fed on New Zealand white rabbits' ears in the preventive veterinary medicine laboratory of Qinghai University and kept in an environmental chamber at 25 ± 1 °C and 90% relative humidity under a 12-h light-dark cycle.

Tick midgut preparation and total RNA extraction

The cylindrical white cotton cloth covered the rabbit's ear, and one end was fixed on the rabbit's ear. A total of 75 adult ticks (15 male and 60 female) were restricted to feeding on the ears of rabbits bound in a cloth bag. Male ticks stimulated female ticks to attach to the host to start feeding and to be inseminated to complete the feeding process. Ticks

were allowed to attach and begin blood feeding on the host. Tick midgut was then collected at 0 h (before the initiation of blood feeding), 24 h, 48 h, 72 h, and 96 h after the start of blood feeding. Fifteen female ticks were collected from rabbit ears at each time point. The same experiment was performed three times, each as a biological replicate. Fifteen midgut samples from the above groupings were prepared for one sample pooling. Three biological replicates were performed for each time point (MG 0A, MG 0B, MG 0C, MG 24A, MG 24B, MG 24C, MG 48A, MG 48B, MG 48C, MG 72A, MG 72B, MG 72C, MG 96A, MG 96B, and MG 96C) (Fig. 1). After the end of the experiment, the rabbits were raised for 2 weeks firstly. Then, the rabbits were fully anesthetized with ketamine (Shanghai Jiedawei Pharmaceutical Technology Development Co., Ltd., Shanghai, China) at 20 mg kg^{-1} by intramuscular injection before being sacrificed.

The basis scapituli of the tick were cut off with a planer and planing tweezers in phosphate-buffered saline (PBS) treated with 1% diethylpyrocarbonate (DEPC) at a low temperature (4 ℃) of pH 7.4. The internal organs of the tick were exposed under a microscope, and the midgut was carefully removed using fine-tipped tweezers. The intestinal tissue was placed into a centrifuge tube, and the centrifuge tube was quickly placed into liquid nitrogen. Forty-five pairs of intestinal tissues were obtained in this study. Total RNA was extracted using TRIzol Reagent (Invitrogen, CA, USA). The quality of the RNA samples was confirmed by using a 2100 Bioanalyzer (Agilent Technologies, Invitrogen, CA, USA).

Tick midgut transcriptome assembly and functional annotation

Then, we constructed the cDNA library of the obtained RNA using the NEBNext® Ultra™ RNA Library Prep Kit for Illumina® (NEB, Ipswich, MA, USA), which contains enzymes and buffers for the preparation of cDNA libraries for next-generation sequencing. The first strand of cDNA was synthesized in the M-MuLV (NEB, USA) reverse transcriptase system using the fragmented mRNA as the template and the random oligonucleotide as the primer, and the second strand of cDNA was synthesized using dNTPs as the raw material.

After the construction of the library, a Qubit 2.0 fluorometer (Life Technologies, Carlsbad, USA) was used for preliminary quantification, and the library was diluted to 1.5 ng/μL. Then, we used an Agilent 2100 bioanalyzer (Agilent Technologies, Invitrogen, CA, USA) to detect the insert size of the library. After the insert size was verified to be within the expected range using an Agilent 2100 bioanalyzer, we performed RT-qPCR to accurately quantify the effective

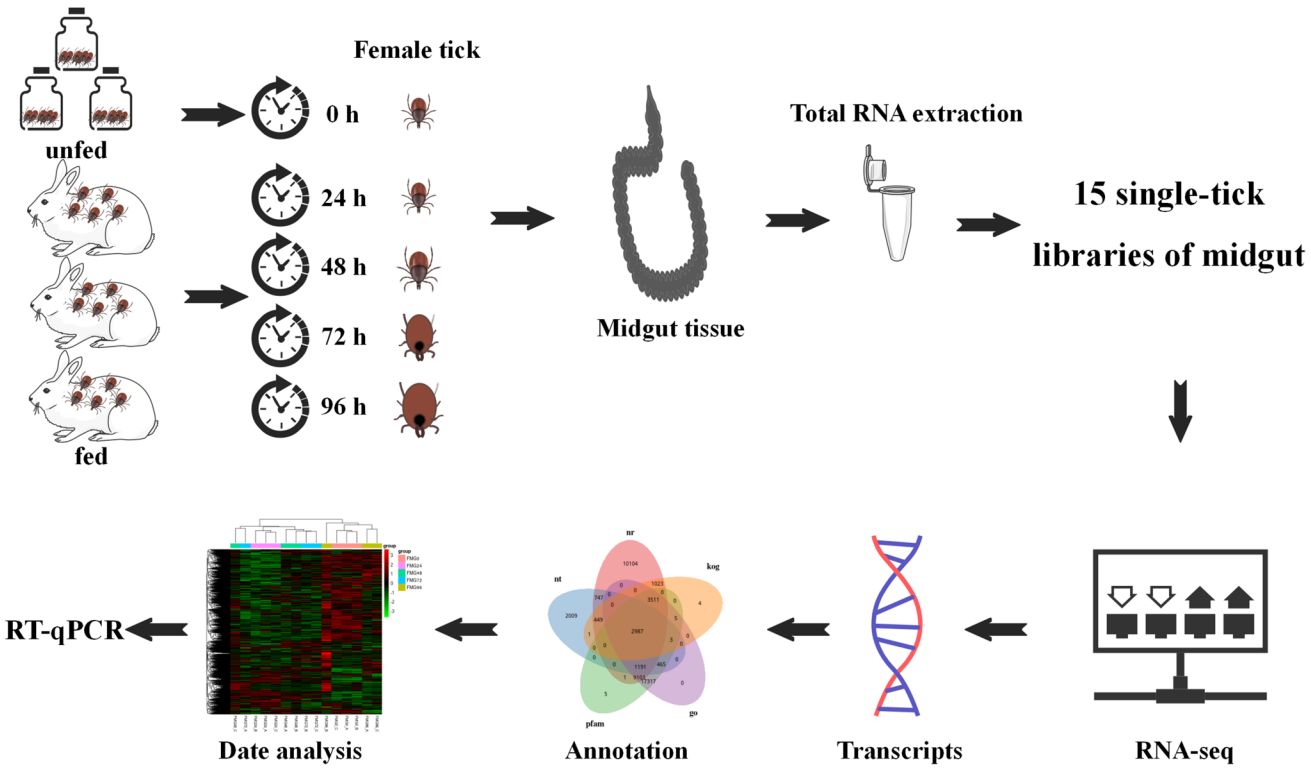

Fig. 1 Schematic illustration of the experimental design. Fifteen female adult ticks were collected from unfed ticks (0 h) and four time points of feeding (24 h, 48 h, 72 h, and 96 h) on the same rabbit (n = 3). The midgut tissue of ticks is isolated. Fifteen midgut tissues were established in a library. Therefore, 15 single-tick libraries of midgut were established

concentration of the library. For successful sequencing, we aimed for an effective library concentration higher than 2 nM, as this concentration ensures an adequate amount of DNA template for the sequencing reaction, thereby guaranteeing the quality of the library. The library was sequenced on an Illumina NovaSeq 6000 platform with 150-base paired-end reads (Novogene Bioinformatics Corporation, Beijing, China).

However, the data in the database contained a small number of reads with sequencing connectors or with low sequencing quality. The original data needed to be filtered to ensure the quality and reliability of data analysis. After removing the rabbit genome sequence using Bowtie2 version 2.2.5 and conducting preliminary quality control, we performed multiple alignments of the raw or clean reads. Fastp (version 0.19.7) is used to clean up raw Illumina data. The read was removed by the adapter, the read containing N was deleted (N indicates that the basic information cannot be determined), and some low-quality reads needed to be removed (the base of Qphred ≤ 20 accounts for more than 50% of the total read length).

After clean reads were obtained, clean reads were spliced to obtain reference sequences for subsequent analysis. Since there is no transcriptome of *D. nuttalli* as a reference, it was necessary to assemble clean reads to obtain reference sequences for future research. Trinity (version 2.8.5) was used to splice clean reads. Trinity combined three independent software modules to process and splice a large number of RNAseq data in turn, including cocoon, chrysalis, and butterfly. During the assembly process using Trinity software, the reads were first clustered based on sequence similarity. Transcripts with shared sequences were grouped together, and then, through a series of algorithms and filtering steps, the redundant transcripts were removed to obtain the unigene set. Therefore, the transcriptome of *D. nuttalli* was reassembled into a clean reading for transcriptome reconstruction.

Based on Trinity splicing, the transcripts were aggregated into many clusters according to the shared reads between transcripts. Combined with transcript expression levels among different samples and the H-Cluster algorithm, transcripts with different expression levels among samples were separated from the original cluster to establish a new cluster. In this way, redundant transcripts can be gathered to improve the detection rate of differentially expressed genes.

Evaluate the quality of assembled transcripts through BUSCO (Benchmarking Universal Single Copy Orthologs). The BUSCO evaluation uses a single copy of a direct Homeotic gene-gene library. BUSCO can evaluate the integrity of assembled transcripts by combining software such as tblastn, augustus, and hmmer (Simão et al. 2015). We use BUSCO software to evaluate the splicing quality of Trinity.fasta, unigene.fasta, and cluster.fasta obtained by splicing. Based on the comparison ratio and completeness, we evaluate the accuracy and completeness of the splicing results.

Comprehensive gene function information was obtained through gene function annotation in seven databases: NCBI nonredundant protein sequences (NR), NCBI nucleotide sequences (NT), Protein family (PFAM), Eukaryotic Orthologous Groups (KOG), Swiss Prot, Kyoto Encyclopedia of Genes and Genomes (KEGG) (Kanehisa and Goto 2000; Kanehisa 2019; Kanehisa et al. 2021), and Gene Ontology (GO). The notes are as follows: NR (diamond v0.8.22 e-value = 1e-5), NT (NCBI blast 2.2.28 + e-value = 1e-5), PFAM HMMER 3.0 package (hmm can e-value = 0.01), Clusters of KOG (diamond version 0.8.22 e-value = 1e-3), Swiss Prot, a manually annotated and reviewed protein sequence database (diamond version 0.8.22 e-value = 1e-5), KEGG (KEGG automatic annotation server e-value = 1e-10), and GO (Blast2GO version 2. 5, e-value = 1e-6). The BLAST alignment parameter was E-value = 1e-5. 19.68% identity cut-off to classify transcripts to NR. 5.3% identity cut-off to classify transcripts to NT. 6.32% identity cut-off to classify transcripts to KEGG. 11.11% identity cut-off to classify transcripts to Swiss Prot. 23.38% identity cut-off to classify transcripts to PFAM. 23.37% identity cut-off to classify transcripts to GO. 5.39% identity cut-off to classify transcripts to KOG. Genes were compared according to the priority order of the NR protein library and the SwissProt protein library. If the information was matched, the open reading frame (ORF) coding box information of transcripts was extracted from the comparison results, and the coding region sequence was translated into an amino acid (aa) sequence (from 5′ to 3′) according to the standard codon table. For the sequences that were not compared with the NR protein library and the SwissProt protein library or the sequences that were not predicted in the comparison, ESTScan (3.0.3) software was used to predict the ORF to obtain the nucleic acid sequence and aa sequence encoded by these genes. ESTScan is a program that can detect coding regions in DNA/RNA sequences, even if their quality is low. ESTScan can also detect and correct sequence errors that cause frameshifts. The missing single gene in BLAST was analyzed by ESTScan to predict its coding region and determine its sequence direction.

Analysis of differentially expressed genes

During the alignment process, we used RSEM software (Li and Dewey 2011), and the Bowtie2 (version 2.25) parameter of RSEM was set to a mismatch of 0 (the default parameter of Bowtie2) (Langmead and Salzberg 2012). RSEM quantified the alignment results of Bowtie2, and the number of reads compared with the gene was used as a read count. FPKM is the expected number of fragments per kilobase of transcript sequence per

millions of base pairs sequenced. FPKM considers the effects of sequencing depth and gene length on fragment count at the same time. For transcriptome data without a reference genome, FPKM > 0.3 was considered to indicate gene expression. After the gene expression amount was obtained, the expression data can be statistically analyzed, and then, the genes with significant differences between different samples can be screened. The analysis of differentially expressed genes (DEGs) is mainly divided into three steps. First, we need to normalize the original read count, the *P* value is then calculated by the statistical model, and the FDR value is obtained through multiple hypothesis testing and correction (BH) (error detection rate, padj is its common form). During the variance analysis, the difference analysis was conducted after standardization through DESeq.

RT-qPCR

To validate the transcriptome sequencing results, the transcriptome results were categorized, from which 10 pairs of DEGs were randomly screened and validated by quantitative real-time PCR (RT-qPCR), respectively. cDNA was synthesized with the RNA of the *D. nuttalli* midgut at unfed ticks (0 h) and four time points of feeding (24 h, 48 h, 72 h, and 96 h). The RNA obtained was diluted to the same concentration, and cDNA was synthesized using the PrimeScript™ RT Master Mix kit (TaKaRa, Japan). The specific primers were designed by GenScript Real-time PCR Primerdesign (https://www.genscript.com/tools real-time-PCR-taxman-primer-design-tool.gen script. com/tools real-time-PCR-taxman-primer-design-tool). *β-Actin* was selected as an internal reference gene. All primers and targeted genes are shown in Additional file 1: Table S1. RT-qPCR was performed using the SYBR™ Green Master Mix kit (Thermo Fisher Scientific, USA) according to the manufacturer's instructions under the following conditions: 50 °C for 2 min and 94 °C for 30 s followed by 30 cycles of 95 °C for 15 s, 56 °C for 15 s, and 72 °C for 20 s in a final volume of 20 µL. RT-qPCR was performed on 96-well plates three times for each reaction, with each reaction representing a biological replicate. A total of three biological replicates were used for each time point (0 h, 24 h, 48 h, 72 h, and 96 h) of *D. nuttalli* midgut samples. The cycle threshold (Ct) values of DEGs were determined by the $2^{-\Delta\Delta Ct}$ method. The correlation analysis was based on a multilevel mixed-effect linear model (Bakdash and Marusich 2017). A correlation analysis between the transcriptome and quantitative real-time PCR data was performed using the online site rmcorrShiny (https://lmarusich.shinyapps.io/shiny_rmcorr/).

Results and discussion

RNA sequencing and de novo assembly of the midgut transcriptome

In this study, we aimed to explore the dynamic changes in gene expression in the midgut during the early stages of blood feeding by adult female *D. nuttalli*. To achieve this, we selected five distinct time points for tick blood feeding. Zero hour represents the starving state of the tick. It offers a reference for subsequent research to comparatively analyze the changes in gene expression during the blood-feeding process. Twenty-four hours is an important stage in the early period of tick blood feeding. The midgut starts to contact and process the newly ingested blood components, and the genes related to the initial blood digestion, nutrient uptake, and immune regulation begin to change in expression to adapt to the new physiological demands. At 48 h, the tick is in the process of continuous blood feeding, and the physiological processes in the midgut further progress. The blood digestion process accelerates, the demand for nutrients increases, and the metabolic activities of the midgut cells become more vigorous. Seventy-two hours is close to the middle and late stages of the early blood-feeding process of *D. nuttalli*, and the processes related to pathogen transmission may also start or intensify. Ninety-six hours represents a stage within the early blood-feeding period where the tick is approaching a relatively advanced stage of blood-meal acquisition, in the context of the initial 4-day sampling window for our study. At this stage, the tick is involved in the recovery after nutrient uptake, preparation for egg laying, or other processes related to physiological adjustment after blood feeding. In this study, to analyze and compare the midgut transcriptomes of *D. nuttalli* female ticks at different blood-feeding times, the RNA was extracted from three replicated biological samples of midgut tissue from each physiological condition, and sequenced, assembled, and annotated the samples on the Illumina HiSeq system.

We obtained the unigene set by utilizing Trinity software to assemble the clean reads, followed by the removal of redundant transcripts through a series of algorithms and filtering steps. Transcripts, on the other hand, are the products of gene transcription and encompass all RNA molecules produced from the genome. They may represent various splicing variants or isoforms of the same gene, as well as transcripts from different genes. A total of 23,493,763, 24,911,811, 21,163,653, 22,319,163, and 22,123,654 raw reads were obtained from the midgut of female ticks that were fed for 0 h, 24 h, 48 h, 72 h, and 96 h by using Illumina sequencing technology. The Q20 values for these reads were 98.02%, 97.99%, 98.05%, 97.77%,

and 97.99%, respectively. After removing reads containing adapters, reads containing poly-N, and low-quality reads, 22,524,912, 23,752,325, 20,377,718, 21,300,710, and 20,378,658 high-quality clean reads were generated for assembly (see Additional file 2: Table S2 for other detailed data). All clean reads were assembled into 287,057 transcripts by Trinity software, with an N50 of 2004 bp. A total of 147,915 unigenes were obtained, with an N50 of 1486 bp. The length distributions of the transcripts and unigenes are shown in Fig. 2, and most of them were 300–500 bp, accounting for 36.96% and 43.73%, respectively. The mean lengths of the transcripts and unigenes were 1201 and 989 bp, respectively. The results of the assembly are listed in Additional file 3: Table S3.

BUSCO software (v5.4.7) is utilized to assess the quality of assembled Trinity.fasta, unigene.fasta, and cluster.fasta. It evaluates the accuracy and integrity of splicing results based on sequence alignment outcomes. The analysis indicates that complete and single copy account for 80.7% in cluster.fasta, 80.7% in unigene.fasta, and 42.9% in Trinity.fasta (Additional file 4: Fig. S1). BUSCO analysis revealed high transcriptome completeness with a low percentage of missing or fragmented reads.

Functional annotation

After all transcripts were obtained, the transcripts were annotated by databases including the NR, NT, KEGG, Swiss Prot, PFAM, GO, and KOG databases. The searches in these databases were conducted on January 2022. In total, 147,915 transcripts were annotated by BLAST searches against public databases. Among these, the number of single genes identified in comparison to Pfam was 34,588 (23.38%), and the number of single genes identified in comparison to GO was 34,582 (23.37%). The number of single genes compared with other databases is shown in Additional file 5: Table S4. The distributions of the E-value (< 1E−60) and similarity (> 80%) blast against the Nr database were 36.7% and 22.7%, respectively. In the database-based species classification, 35.7% of the single genes were matched with *I. scapularis*, and the percentages of the single genes consistent with *Nuttelliella namaqua*, *Centruroides sculpturatus*, *Limulus polyphemus*, and *Apostichopus japonicus* were 6.8%, 5.5%, 4.3%, and 2.7%, respectively (Additional file 6: Fig. S2).

Functional classification

A total of 34,582 unigenes were annotated into 42 subcategories belonging to three GO terms. The functions of these genes were classified according to biological processes, cell components, and molecular functions. The top three subclasses of unigenes included cellular processes, binding genes, and cellular analytical entity (Additional file 7: Fig. S3). All assembled unigenes were also aligned with the KOG database resulting in the functional classification of 8970 unigenes into 26 categories. The largest group consisted of unigenes with general function predictions only, totaling 1744 unigenes (19.44% of all KOG annotated unigenes), followed by a group of signal transduction mechanisms (n = 970) and a group related to post-translational modifications, protein turnover, and chaperones (n = 330). Collectively, 39.53% of unigenes in the first three categories were annotated in the KOG database. The smallest group was related to cell movement, comprising 17 unigenes (0.19%) (Additional file 8: Fig. S4). Based on the KEGG database, the biological pathways and gene interactions of single genes were analyzed. A total of 10,093 unigenes were divided into five categories (Cellular Processes, Environmental Information Processing, Genetic Information Processing, Metabolism, and Organismal Systems). The first three KEGG pathways

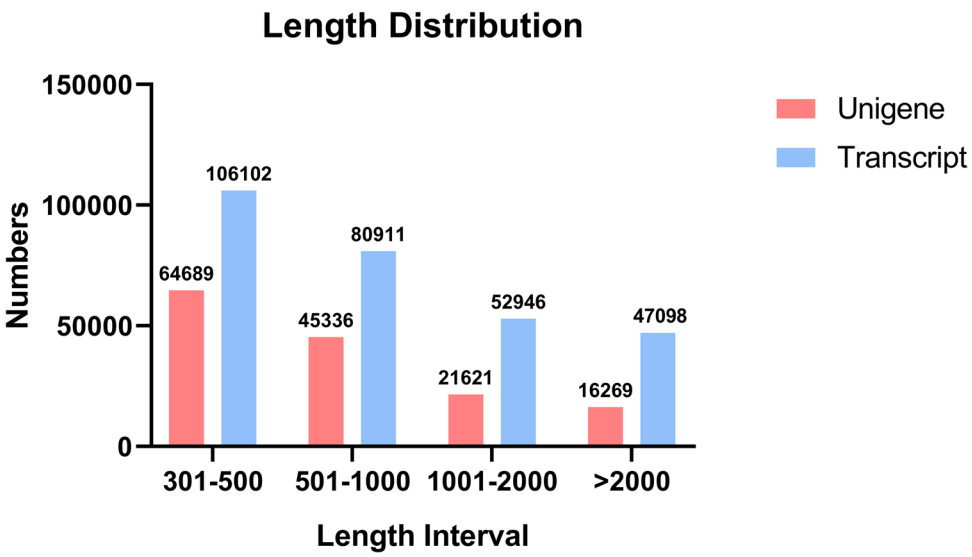

Fig. 2 The length distribution of the unigenes and transcripts. The abscissa is the length interval, and the ordinate is the number of transcripts/unigene in each size category. Blue indicates unigene and red indicates transcripts

were signal transduction ($n = 1101$, 10.91%), transport and catabolism ($n = 907$, 8.00%), and endocrine system ($n = 617$, 6.11%) (Additional file 9: Fig. S5).

Differential expression analysis of the midgut transcriptomes at different blood feeding times

The gene expression of the *D. nuttalli* tick was significantly different under starvation and different blood feeding periods. Differential gene expression of significantly up-regulated ($|\text{Log}_2$ fold change$| \geq 1$, adjusted $p \leq 0.05$) or down-regulated ($|\text{Log}_2$ fold change$| \leq 1$, adjusted $p \leq 0.05$) transcripts were determined using the software DESeq2 (Love et al. 2014). There were 4572 differentially upregulated genes and 6416 differentially downregulated genes in the unfed and blood feeding groups at 24 h. There were 1510 upregulated genes and 3344 downregulated genes compared with the blood feeding for 48 h and unfed groups. In a comparison between the unfed and blood feeding for 72 h groups, 2065 genes were down-regulated, and 4356 genes were upregulated. When ticks did not suck blood or sucked blood for 96 h, the number of upregulated genes was 1118, and the number of downregulated genes was 2020. There were 1453 upregulated genes and 1209 downregulated genes in the 24 h blood feeding group compared with the 48 h blood feeding group. There were 741 upregulated genes and 753 downregulated genes in the 24 h blood feeding group compared with the 72 h blood feeding group. There were 3339 upregulated genes and 2938 downregulated genes in groups with blood feeding for 24 h and 96 h, respectively. In a comparison of the 72 h and 96 h blood feeding groups, the upregulated genes were 103 and 681, respectively, and the downregulated genes were 75 and 366, respectively. There were 1190 upregulated genes and 490 downregulated genes after 72 h of blood feeding compared with 96 h of blood feeding (Additional file 10: Fig. S6).

We classified and counted the differentially expressed genes of *D. nuttalli* at different blood feeding times to better understand the dynamic changes in gene expression in the midgut during the early stages of blood collection from *D. nuttall* (Additional file 11: Table S5). Based on the analysis of differentially expressed genes (DEGs) in *D. nuttalli* at different blood feeding time points, we can infer several physiological processes. At 0 h, the tick is non-blood feeding, with certain basal metabolic and life-sustaining processes still active, as indicated by the relatively high number of genes associated with "other proteases and miscellaneous proteins" to 24 h post-blood feeding, the upregulation of "immunogenic proteases" and "transporters" suggests the initiation of blood digestion and active nutrient uptake. Meanwhile, the downregulation of many genes in "other proteases and miscellaneous proteins" indicates a shift away from non-feeding-related physiological activities. Between 24 h and 48 h, the continuous upregulation of "immunogenic proteases" and "transporters" along with the downregulation of "protease inhibitors" indicates that the processes of blood digestion and nutrient uptake not only continue but also intensify. The changes in "other proteases and miscellaneous proteins" further suggest an adjustment in protease-related physiological activities in the midgut. From 48 to 72 h, the continuous increase in "transporters" indicates that the tick is consistently absorbing nutrients, likely due to its increasing demands for growth, development, and reproduction as the duration of blood feeding extends. The significant changes in "protease inhibitors" and "other proteases and miscellaneous proteins" suggest that blood digestion and related metabolic processes are ongoing and becoming more complex. At 96 h, the upregulation of "ribosomal function proteins" indicates that the tick is actively synthesizing proteins, which may be associated with physiological adjustments such as egg-laying or adaptations to post-feeding metabolic changes. The persistent changes in "immunogenic proteases" and "other proteases and miscellaneous proteins" suggest that blood digestion and midgut-related protease activities remain in a dynamic state of adjustment to meet the tick's physiological needs during the later stages of blood feeding. In summary, throughout the blood-feeding process, the tick undergoes a series of complex and coordinated physiological changes to adapt to its new nutritional environment and support its survival and reproduction.

A volcano plot was constructed to illustrate the DEGs across various blood-feeding time intervals (Fig. 3). These plots effectively highlight the significant differences in the number of DEGs between different blood-feeding time periods. The findings indicate that the midgut plays an important role in the blood-feeding process of ticks. To confirm the reliability of the transcriptome data, 10 DEGs were selected by qRT-PCR. The qRT-PCR results confirmed that the expression patterns of the studied transcripts exhibited trends similar to those observed in RNA-seq analysis (Fig. 4A), although the change amplitude of the expression multiples between the two methods may be different. Despite variations in the magnitude of the fold-change values, both methods yielded consistent results that demonstrated a direct correlation ($R^2 = 0.194$, 95% CI [−0.658, −0.153], $p<0.01$, Fig. 4B). In conclusion, the results showed the reliability and accuracy of transcriptome expression analysis based on RNA sequencing.

D. nuttalli tick midgut proteases and protease inhibitors

In this study, the protease-like molecules in *D. nuttalli* were noted by midgut transcriptome assembly and functional annotation. Proteases play an important role involved in many biological functions, including development,

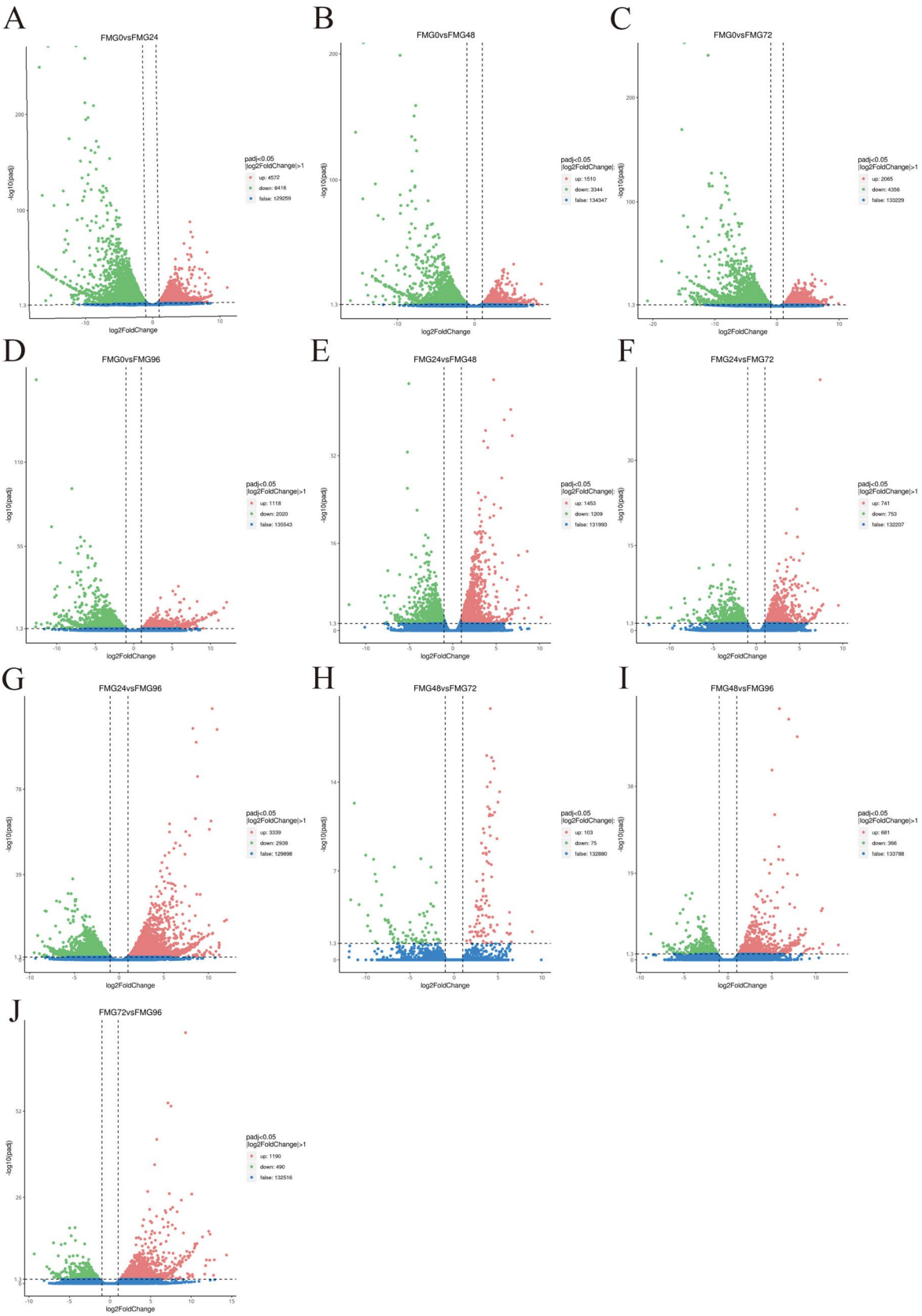
A
FMG0vsFMG24
padj<0.05
|log2FoldChange|>1
up: 4572
down: 6416
false: 129259
B
FMG0vsFMG48
padj<0.05
|log2FoldChange|>1
up: 1510
down: 3344
false: 134347
C
FMG0vsFMG72
padj<0.05
|log2FoldChange|>1
up: 2065
down: 4356
false: 133229
D
FMG0vsFMG96
padj<0.05
|log2FoldChange|>1
up: 1118
down: 2020
false: 135543
E
FMG24vsFMG48
padj<0.05
|log2FoldChange|>1
up: 1453
down: 1209
false: 131993
F
FMG24vsFMG72
padj<0.05
|log2FoldChange|>1
up: 741
down: 753
false: 132207
G
FMG24vsFMG96
padj<0.05
|log2FoldChange|>1
up: 3339
down: 2938
false: 129898
H
FMG48vsFMG72
padj<0.05
|log2FoldChange|>1
up: 103
down: 75
false: 132880
I
FMG48vsFMG96
padj<0.05
|log2FoldChange|>1
up: 681
down: 366
false: 133788
J
FMG72vsFMG96
padj<0.05
|log2FoldChange|>1
up: 1190
down: 490
false: 132516
-log10(padj)
log2FoldChange

◂**Fig. 3** Statistics of DGEs in *D. nuttalli* midgut at different blood feeding time points. **A** Volcano map of DEGs between no feeding (0 h) and after 24 h of blood feeding. **B** Volcano map of DEGs between no feeding (0 h) and after 48 h of blood feeding. **C** Volcano map of DEGs between no feeding (0 h) and after 72 h of blood feeding. **D** Volcano map of DEGs between no feeding (0 h) and after 96 h of blood feeding. **E** Volcano map of DEGs between 24 h and 48 h of blood feeding. **F** Volcano map of DEGs between 24 h and 72 h of blood feeding. **G** Volcano map of DEGs between 24 h and 96 h of blood feeding. **H** Volcano map of DEGs between 48 h and 72 h of blood feeding. **I** Volcano map of DEGs between 48 h and 72 h of blood feeding. **J** Volcano map of DEGs between 72 h and 96 h of blood feeding

apoptosis, homeostasis, reproduction, and host defense (Puente et al. 2005). During and after blood feeding, the proteins in the blood are digested by the proteases present in the midgut. As mentioned above, blood digestion is a slow process that occurs in the acidic environment of the inner vesicles of midgut cells, facilitated by cathepsin-like, papain-like, and other proteases in ticks.

To date, among the 233 identified *I. scapularis* proteases with putative activity, the cysteine, metalloproteinase, and serine proteases are approximately 19% (44/233), 40% (93/233), and 28.3% (66/233), respectively (Mulenga and Erikson 2011). In the present study, the overlapping sequences were preliminarily classified as aspartic proteases, serine proteases such as cathepsins, metalloproteases, and glutathione peroxidases. Cysteine proteases, in particular, play a crucial role in the early stages of tick blood feeding. They function by degrading extracellular matrix proteins, such as collagen, thereby facilitating the penetration of the tick's mouthparts into the host's skin (Francischetti et al. 2003). For instance, Cluster-36782.63977 exhibited the highest expression level at 24 h, providing further evidence of this role.

This study analyzed the changes in digestive proteinases of *D. nuttalli* at various blood-feeding times. By comparing time points such as 0 h with 24 h, 48h, 72h, and 96 h, significant differences were observed in the number of upregulated and downregulated genes associated with cysteine proteases aspartic proteases, serine proteases, and metalloproteases. In the comparison between 0 h and 48 h time points, 11 genes were upregulated while 23 were downregulated. The number of upregulated genes was relatively lower than that observed at 24 h, suggesting that changes in enzyme expression may slow down or follow a different pattern as blood-feeding progresses. At 72 h, compared to 0 h, 13 genes were upregulated and 38 were downregulated. Notably, a significant number of downregulated metalloprotease genes were identified, indicating that the function of metalloproteases may be strongly regulated during this period. In contrast, the metalloprotease listed in Table 1 showed relatively minor variations across different time points. Nevertheless, previous research has demonstrated its potential as a target for anti-tick vaccines.

Interestingly, aspartic proteases are uniquely expressed in the intestinal tract of ticks rather than in their eggs, highlighting their significance as key proteases for blood digestion (Sojka et al. 2008). Notably, it has been reported that cysteine and aspartic proteases can synergistically digest host blood proteins. Moreover, both cysteine and aspartic proteases have emerged as promising targets for anti-tick vaccines (Song et al. 2022; Sojka et al. 2008). However, in this study, its expression level decreased during the tick's blood-feeding process. These findings may provide new insights for future research on *D. nuttalli* (Additional file 12: table S6).

Consequently, analyzing the differentially expressed genes in the midgut tissues of female ticks at various stages of blood feeding holds great promise for developing novel strategies to disrupt tick feeding and inhibit pathogen transmission.

However, to avoid over-hydrolysis of protease molecules, ticks have accordingly developed a variety of protease hydrolysis inhibitory mechanisms (Xavier et al. 2019; Sun et al. 2019; Miyoshi et al. 2010; Miyoshi et al. 2007). In this study, the protease inhibitors were identified and annotated, such as chymotrypsin elastase inhibitor, cysteine protease inhibitor, Kunitz protease inhibitor, serine protease inhibitor, and translation initiation inhibitor. Notably, chymotrypsin-elastase inhibitor, cysteine protease and A protease inhibitor, and serine protease inhibitor were expressed at higher levels in the midgut at 24 and 48 h, which show that these proteins may regulate the early stage of tick feeding (Table 1). The expression of these inhibitors in different blood-feeding periods was different in the current tick midgut, which may be that the expression of some proteases in the midgut of female ticks increases with the blood feeding. This may be because proteases and inhibitors show a dynamic equilibrium state in different blood-feeding periods, such as Cathepsin could help ticks maintain blood meal fluidity for extended feeding periods (Xavier et al. 2019).

Generally, the serine protease inhibitor (serpin) and kunitz-type protease inhibitor has been considered to play a key role in the interaction between ticks and hosts, such as regulating the coagulation cascade, clot lysis, inflammation, response, and complement activation (Mulenga et al. 2009; Gettins 2002; Huntington 2006; Silverman et al. 2001; Silverman et al. 2004). Hence, serpin and kunitz-type protease inhibitor were common as a target in immune response during host bit by ticks, such as serpin was used to develop an anti-tick vaccine which increased tick mortality in rabbit anti-tick studies (Imamura et al. 2005; Ma et al. 2023a, b). In addition, chymotrypsin elastase inhibitors, cysteine protease inhibitors, and translation initiation inhibitors were also identified in the current analysis. However, further research is needed to determine their relationship to the blood meal digestion of *D. nuttalli* (Table 1). Chymotrypsin-elastase

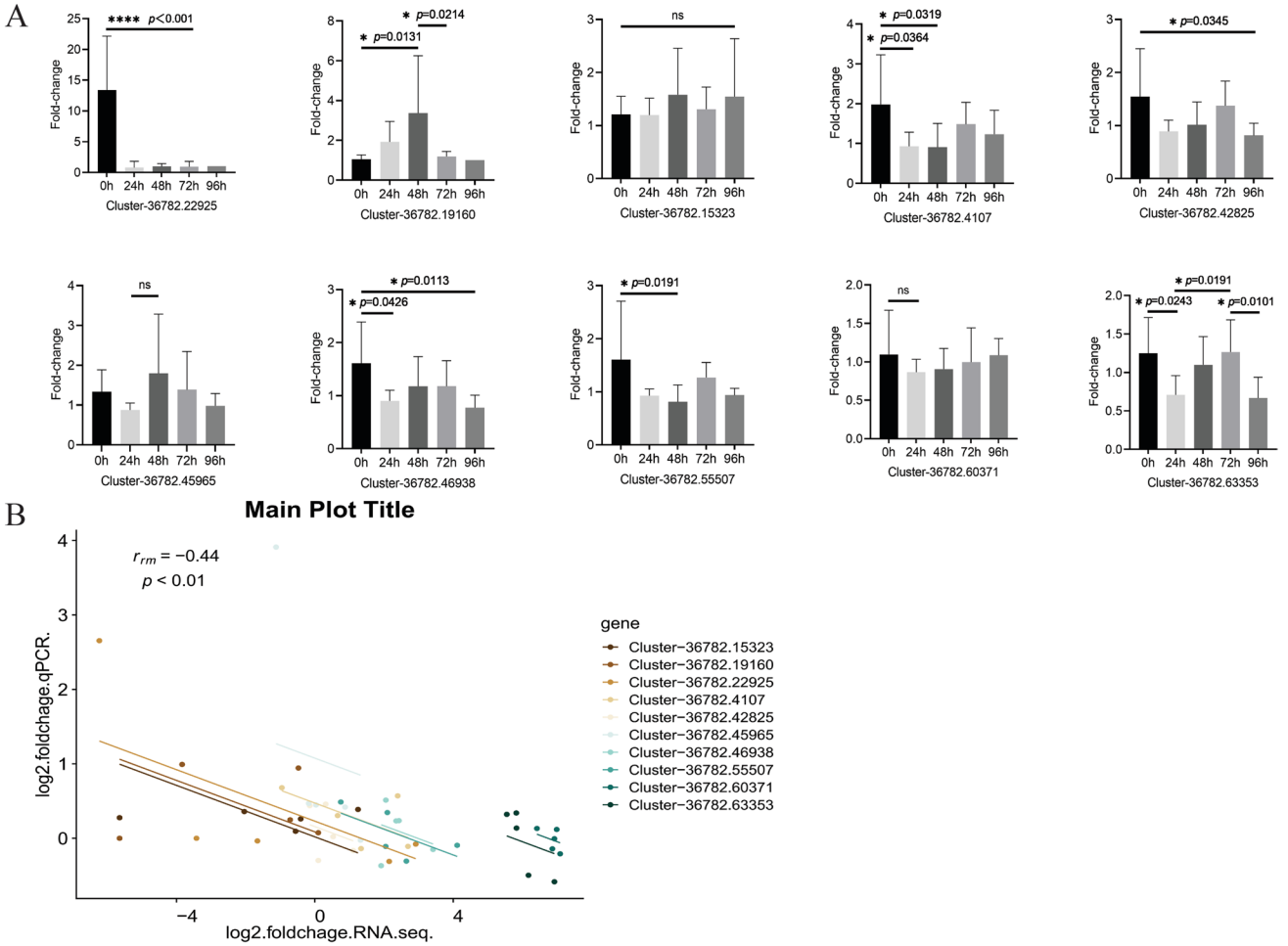

Fig. 4 **A** RT-qPCR validation of selected 10 differentially expressed genes (DEGs). RT-qPCR was performed using cDNA templates derived from female *D. nuttalli* ticks with 0h, 24h, 48 h, 72 h, and 96 h of blood feeding. The transcript expression levels of the selected genes were normalized to that of the *β-actin* housekeeping gene. Statistical comparison across all time points for each parameter was performed using a one-way ANOVA followed by post hoc tests (Tukey's test). $*P < 0.1$. $****P < 0.0001$. ns, no significant difference. **B** Correlation between values of the $\log_2$ (fold-change) obtained from RT-qPCR and RNA-seq for the selected genes. The *x*-axis indicates the $\log_2$ (fold-change) according to the RNA-seq data, and the *y*-axis indicates the $\log_2$ (fold-change) according to the RT-qPCR data

inhibitor ixodidin (Cluster-36782.85225) shows a remarkable increase in expression at 72 h. As a protease inhibitor, it controls the proteolytic process in the tick. By inhibiting related proteases, it prevents over-destination, thus maintaining the balance of protein metabolism. This is especially crucial during the rapid-feeding stage, as it ensures the tick digests blood in an organized way and protects its own tissues from damage.

D. nuttalli tick midgut transporters and ligand binding proteins

In this study, an initial identification of *Dermacentor nuttalli* midgut transporters and/or binding proteins was carried out, and they were categorized into overlapping groups as presented in Table 2. Among the 442 proteins detailed in Table S7 and Table 2, a notable subset of 20 were annotated as ABC transporters. Interestingly, *D. nuttalli*, like many other organisms, exhibits a pattern of selective expression modulation of these proteins during specific time intervals. Notably, the ABC transporters were found to reach their peak expression level at 24 h post-initiation of tick feeding. This temporal correlation suggests a potential functional connection between the increased expression of ABC transporters and the early stages of the tick feeding process.

Cyclosporine A, a member of the ATP-binding cassette (ABC) transporter family, has been shown in previous studies (Lara et al. 2015; Mangia et al. 2018; Mate et al. 2022; Pohl et al. 2011) to play a significant role in the detoxification of amitraz and ivermectin during the blood meal. These chemicals are well-known for their involvement in the development of tick resistance to acaricides. Additionally, it has

Table 1 Partially DEGs of *D. nuttalli* tick midgut proteases and protease inhibitors

Accession	Annotation	Gene length (bp)	*E* value	FPKM values Feeding time point									
				0 h	SD	24 h	SD	48 h	SD	72 h	SD	96 h	SD
Proteases													
Cluster-36782.23289	Aspartic protease, putative [*Dermacentor variabilis*]	800	5.5E-104	0.92	0.36	795.54	123.66	155.01	34.53	402.79	285.00	11.06	5.35
Cluster-36782.92640	Serine protease protein [*Dermacentor variabilis*]	1183	3.80E-08	0.25	0.12	24.78	6.27	32.64	13.15	33.56	17.52	35.92	9.51
Cluster-36782.64082	Cathepsin B endopeptidase, putative [*Ixodes scapularis*]	1477	2.60E-155	898.35	16.99	3192.24	105.294	2284.48	400.19	2531.01	128.59	1586.70	219.23
Cluster-36782.70733	Cathepsin C, putative [*Ixodes scapularis*]	4919	1.70E-09	7.09	0.50	2.82	0.30	2.42	0.37	2.38	0.46	3.96	1.17
Cluster-36782.64169	Cathepsin L [*Rhipicephalus haemaphysaloides*]	1373	9.00E-163	52.73	7.60	117.41	3.17	124.82	27.58	95.09	23.22	61.28	27.98
Cluster-36782.63977	Cathepsin L-like cysteine proteinase [*Dermacentor variabilis*]	2737	5.20E-69	316.09	16.95	1720.89	368.73	592.30	180.49	1012.14	171.59	697.00	241.69
Cluster-36782.12183	Metalloprotease 1 [*Rhipicephalus microplus*]	1277	7.20E-106	0.00	0.00	0.05	0.07	0.48	0.68	1.08	0.61	0.16	0.23
Cluster-36782.63168	Metalloprotease TIKI1-like [*Centruroides sculpturatus*]	2866	3.40E-119	9.48	1.14	2.60	0.46	3.94	0.42	2.34	0.43	3.93	0.84
Cluster-36782.55355	Glutathione peroxidase [*Dermacentor variabilis*]	6128	5.00E-19	12.53	0.44	17.82	1.95	21.36	2.59	18.28	2.37	20.15	2.72
Protease inhibitors													
Cluster-36782.85225	Chymotrypsin-elastase inhibitor ixodidin [*Ixodes scapularis*]	1103	9.30E-09	13.43	2.18	16.82	7.21	11.12	4.40	9.78	6.21	1.47	0.65
Cluster-36782.86537	Cysteine protease and A protease inhibitor, putative [*Ixodes scapularis*]	1830	1.60E-106	3.17	0.91	45.05	5.53	14.85	2.72	8.06	0.91	14.24	3.86
Cluster-36782.20495	Kunitz-type protease inhibitor 2-like [*Cynoglossus semilaevis*]	436	2.10E-12	0.10	0.15	6.95	1.50	25.46	18.49	16.40	15.36	6.80	6.46
Cluster-36782.56896	Serine protease inhibitor 1 RmS-1 [*Rhipicephalus microplus*]	1907	3.10E-145	17.42	4.42	28.43	2.63	20.62	2.01	22.90	6.69	19.50	3.50
Cluster-36782.30380	Serine protease inhibitor 12 RmS12 [*Rhipicephalus microplus*]	2289	1.30E-201	1.59	1.74	0.15	0.06	0.79	1.06	0.23	0.24	1.64	2.19
Cluster-36782.83729	Serine protease inhibitor 16 RmS16 [*Rhipicephalus microplus*]	2589	3.40E-126	2.02	0.58	0.74	0.41	0.74	0.29	0.36	0.26	0.88	0.09
Cluster-36782.83364	Serine protease inhibitor 17 RmS17 [*Rhipicephalus microplus*]	1720	2.90E-142	12.70	9.47	3.96	0.74	4.80	0.28	1.93	0.91	12.57	6.10
Cluster-36782.20856	Translation initiation inhibitor UK114/IBM1, putative [*Ixodes scapularis*]	519	1.40E-34	1.84	2.14	11.31	6.18	14.36	6.65	1.16	1.33	6.77	5.25

SD standard deviation. FPKM values are the mean of the three biological replicates analyzed from each physiological condition and other information see Additional file 13: Table S7

been reported that Cyclosporine A is crucial for the uptake of heme by ticks (Lara et al. 2015; Mangia et al. 2018), further highlighting its importance in tick physiology.

Furthermore, a significant portion of the *D. nuttalli* midgut proteins listed in Table 2 has been previously identified in other research studies. This overlap suggests that these proteins may play integral roles in the complex interaction network of transporter molecules between the host and the tick. Specifically, metal transporters have been proposed to exert a regulatory influence on the virulence factors of tick-borne pathogens (Troxell and Yang 2013; Upadhyay et al. 2014). This regulation could potentially affect the pathogens' ability to establish an infection within the tick and subsequently transmit it to the host. Conversely, ligand-binding proteins may actively participate in the host's coagulation process (Xu et al. 2013; Lee et al. 2019), potentially enhancing the tick's ability to feed and evade host immune responses.

D. nuttalli tick midgut ribosomal function proteins

Ribosomes, essential organelles within cells, are responsible for protein synthesis. Composed of ribosomal RNA (rRNA) and ribosomal proteins, they play a multifaceted and indispensable role throughout the tick life cycle. This study conducted a meticulous examination to identify the overlapping group of ribosomal proteins in the midgut of female *D. nuttalli* ticks at specific time points: 0, 24, 48, 72, and 96 h after blood feeding (Table 3). Notably, Cluster-36782.33624 exhibited high levels of identity, with 99.22%, 85.35%, and 80.23% similarity to *Dermacentor silvarum*, *Rhipicephalus sanguineus*, and *I. scapularis*, respectively. Additionally, Cluster-36782.10886 shared an exact 100% identity with *Aythya fuligula*, while Cluster-36782.59362 had a perfect match with *D. silverum*.

Previous in-depth analyses have revealed that during the blood-feeding process of *D. nutalli*, the organism is compelled to synthesize and secrete a diverse array of proteins that perform essential functions, such as anticoagulation and immunomodulation. Ribosomal proteins play a crucial role in ensuring the accurate and efficient synthesis of these proteins. Consequently, the expression levels of ribosomal proteins exhibit significant variations across different stages of the blood-feeding process. For instance, prior research has firmly established that silencing the ribosomal protein P0 gene in *Haemaphysalis longicornis* is lethal. Furthermore, the application of vaccines based on the P0 protein in ticks has resulted in a substantial increase in mortality rates and a significant reduction in hatchability (Gong et al. 2008; Rodríguez-Mallon et al. 2012).

In this study, RPS-27 was identified as another crucial ribosomal protein. Interestingly, a previous study demonstrated that RPS-27 plays a pivotal role in both the feeding and reproduction of ticks. Specifically, silencing the expression of RPS-27 in *H. longicornis*, it resulted in a significant decline in feeding ability and a marked reduction in engorgement weight after a blood meal (Rahman et al. 2020). However, despite these findings, further comprehensive research is urgently needed to investigate whether other ribosomal protein genes can be precisely targeted as potential candidates for effectively eradicating ticks and curbing their reproductive capabilities.

D. nuttalli tick midgut heat shock proteins

Heat shock proteins (HSPs), recognized as highly conserved "molecular chaperones," possess the remarkable ability to engage in a multitude of intricate and essential functions within cells. In this study, Table 4 presents a curated selection of HSPs identified in the midgut of *D. nuttalli*, providing a valuable overview of their presence. HSPs are integral to cellular machinery, as they facilitate the recovery of cells and their physiological functions following various stressors. Specifically in ticks, HSPs endow the organism's capacity to withstand environmental challenges, a phenomenon well-documented in previous research (Tutar and Tutar 2010; Schlesinger 1990; Villar et al. 2010).

Notably, previous investigations have revealed the involvement of specific HSPs in the response of *I. scapularis* ticks to the stress induced by blood feeding (Benoit et al. 2011). Furthermore, evidence suggests that certain HSPs can exert a modulatory effect on microorganisms, either by directly killing them or inhibiting their growth and activity (Sonenshine and Macaluso 2017). However, despite these significant findings, our understanding of the complete repertoire of HSPs in *D. nuttalli* remains far from comprehensive.

D. nuttalli tick midgut other proteins

In this study, a large number of miscellaneous genes were identified and detailed in the accompanying table. These genes likely play significant yet currently undefined roles in the biological processes of *D. nuttalli.* The unannotated and unknown sequences in the tick transcriptome, as indicated by this table, are highly representative. They may potentially be involved in unique physiological mechanisms specific to *D. nuttalli*, such as its blood-feeding behavior, adaptation to the host, or immune evasion strategies.

An interesting finding is the upregulation of Salp 25D, a homolog of glutathione peroxidase, in both the midgut and salivary glands of *I. scapularis* during blood feeding (Das et al. 2001). Notably, a previous study indicated that silencing Salp 25D in tick salivary glands could impact the

Table 2 Partially *D. nuttalli* tick midgut transporters and ligand binding proteins

Accession	Annotation	Gene length (bp)	*E* value	FPKM values Feeding time point									
				0 h	SD	24 h	SD	48 h	SD	72 h	SD	96 h	SD
Transporters													
Cluster-36782.51837	ABC transporter, putative [*Ixodes scapularis*]	2573	4.80E-117	1.77	1.01	20.22	4.04	5.19	0.38	9.85	6.66	4.06	0.60
Cluster-36782.56628	ABC C2 transporter, partial [*Rhipicephalus microplus*]	1624	3.40E-23	1.18	0.58	1.80	0.07	1.54	1.32	0.75	0.58	0.10	0.11
Cluster-36782.84864	Acetyl-coenzyme A transporter, putative [*Ixodes scapularis*]	2905	4.30E-231	4.44	1.07	4.89	0.24	2.41	0.34	2.89	1.72	3.77	0.41
Cluster-36782.100264	Amino acid transporter, putative [*Ixodes scapularis*]	1690	1.60E-97	0.01	0.02	0.01	0.01	0.88	1.19	0.24	0.31	2.11	2.98
Cluster-36782.79637	Cationic amino acid transporter 3 [*Parasteatoda tepidariorum*]	5701	5.20E-172	5.65	1.99	25.77	2.40	9.83	0.81	9.83	2.07	8.37	2.49
Cluster-36782.58855	Copper transporter, putative [*Ixodes scapularis*]	4090	1.10E-17	4.65	1.22	20.51	5.32	7.67	1.56	8.97	2.02	11.85	3.29
Cluster-36782.49224	Equilibrative nucleoside transporter 2 [*Galendromus occidentalis*]	3673	6.40E-38	3.01	0.71	7.58	1.27	4.12	0.90	3.47	1.31	5.95	1.11
Cluster-36782.58075	Glutamate transporter, putative [*Ixodes scapularis*]	710	9.80E-12	3.65	3.30	1.54	0.44	6.18	3.28	8.72	2.94	2.75	1.58
Cluster-36782.69863	H(+)/Cl(−) exchange transporter 7 [*Cryptotermes secundus*]	4418	1.50E-238	8.23	2.49	16.06	1.65	8.34	1.49	8.75	2.41	7.05	1.20
Cluster-36782.93432	Lysine histidine transporter 1 [*Toxocara canis*]	3550	1.70E-11	0.44	0.11	1.03	0.73	0.50	0.31	1.61	0.65	0.67	0.48
Cluster-36782.64452	monocarboxylate transporter, putative [*Ixodes scapularis*]	3835	1.20E-87	12.99	1.68	93.79	14.03	13.16	1.13	39.91	39.78	31.54	15.20
Cluster-36782.23428	Na+/dicarboxylate, Na+/tricarboxylate and phosphate transporter, putative, partial [*Ixodes scapularis*]	1062	1.10E-06	1.82	1.08	0.15	0.16	0.60	0.23	0.15	0.11	0.31	0.22
Cluster-36782.55941	Organic anion transporter, putative [*Ixodes scapularis*]	2471	2.10E-37	2.84	0.21	8.11	1.37	5.94	0.74	4.50	1.22	7.92	2.28
Cluster-36782.66977	Sugar transporter, putative [*Ixodes scapularis*]	3219	7.70E-88	10.01	1.23	2.01	0.68	0.97	0.48	2.02	0.49	1.04	0.45
Ligand binding													
Cluster-36782.55037	Adaptin ear-binding coat-associated protein, putative [*Ixodes scapularis*]	1931	5.60E-86	9.86	1.59	23.08	0.90	15.28	3.97	16.10	4.22	15.82	5.76
Cluster-36782.61849	Amyloid beta A4 precursor protein (APP)-binding protein, putative, partial [*Ixodes scapularis*]	4497	3.40E-126	30.09	4.71	8.29	1.81	17.19	1.14	14.93	4.62	13.10	1.19
Cluster-36782.34172	Calcineurin-binding protein cabin-1-like [*Centruroides sculpturatus*]	6959	3.50E-279	2.12	0.26	0.84	0.04	0.58	0.13	0.57	0.12	1.04	0.40

Table 2 (continued)

Accession	Annotation	Gene length (bp)	*E* value	FPKM values Feeding time point									
				0 h	SD	24 h	SD	48 h	SD	72 h	SD	96 h	SD
Cluster-36782.85025	Calcium-binding mitochondrial carrier protein Aralar1, partial [*Stegodyphus mimosarum*]	1484	6.40E-21	1.04	0.22	0.06	0.06	0.24	0.17	0.42	0.19	0.60	0.22
Cluster-36782.60033	Calmodulin-binding transcription activator, putative, partial [*Ixodes scapularis*]	11822	2.40E-179	3.61	2.31	0.76	0.08	1.92	0.50	1.50	0.47	2.29	0.19
Cluster-36782.38943	Cysteine-rich protein 2-binding protein isoform X2 [*Lingula anatina*]	2962	5.70E-154	3.12	0.38	0.20	0.04	2.31	2.03	1.77	0.92	4.04	3.61
Cluster-36782.42063	Fatty acid-binding protein, liver [*Anas platyrhynchos*]	488	4.50E-64	9.06	4.35	11.99	15.82	2.50	1.73	1.43	0.76	0.00	0.00
Cluster-36782.41646	Guanylate-binding protein 2-like [*Centruroides sculpturatus*]	3616	1.20E-169	4.12	0.46	15.60	1.68	5.83	1.34	8.29	3.18	5.09	1.20
Cluster-36782.23128	HSP70 binding protein, putative [*Ixodes scapularis*]	1695	1.40E-75	0.36	0.12	10.53	5.11	4.29	3.14	2.53	1.81	0.78	1.11
Cluster-36782.60996	Insulin-like growth factor binding protein-related protein 6 long [*Amblyomma americanum*]	875	4.90E-21	118.15	67.01	5.10	1.16	1.23	1.08	1.56	0.55	1.56	60.84

SD standard deviation. FPKM values are the mean of the three biological replicates analyzed from each physiological condition and other information see Additional file 14: Table S8

Table 3 Partially *D. nuttalli* tick midgut ribosomal function proteins

Accession	Annotation	Gene length (bp)	*E* value	FPKM values Feeding time point									
				0 h	SD	24 h	SD	48 h	SD	72 h	SD	96 h	SD
Cluster-36782.33624	39S ribosomal protein L23, putative [*Ixodes scapularis*]	518	8.90E-55	28.50	4.51	52.59	4.58	35.70	8.83	35.16	16.16	32.38	18.20
Cluster-36782.10886	40S ribosomal protein S10 [*Patagioenas fasciata monilis*]	556	1.60E-73	3.21	1.81	0.84	0.40	0.81	0.85	1.03	1.04	0.00	0.00
Cluster-36782.59362	40S ribosomal protein S27-like, partial [*Sarcophilus harrisii*]	2381	9.30E-14	122.82	20.67	48.79	9.85	39.71	6.21	47.84	6.45	35.68	4.32
Cluster-36782.11475	40S ribosomal protein S3a [*Gallus gallus*]	830	1.50E-141	2.99	2.15	0.31	0.22	1.66	1.88	0.43	0.38	0.00	0.00
Cluster-36782.84519	40s ribosomal protein s6 [*Limosa lapponica baueri*]	803	9.10E-115	2.29	2.29	0.57	0.51	1.22	1.73	0.41	0.06	0.00	0.00
Cluster-36782.63826	60S acidic ribosomal protein P1, putative, partial [*Ixodes scapularis*]	679	5.50E-28	2144.31	109.47	2163.26	192.94	1961.78	260.39	2130.53	280.61	1079.56	169.52
Cluster-36782.31510	60S ribosomal protein L28 isoform X2 [*Nannospalax galili*]	478	2.80E-50	5.38	4.68	2.34	2.02	2.01	2.23	1.22	0.87	0.00	0.00
Cluster-36782.67157	Nucleolar pre-ribosomal-associated protein 1-like [*Limulus polyphemus*]	6505	1.80E-83	11.05	4.05	1.06	0.10	2.95	0.39	2.20	0.22	5.77	0.74
Cluster-36782.62778	Ribosomal pseudouridine synthase, putative [*Ixodes scapularis*]	950	1.50E-39	76.05	5.30	7.22	1.46	11.59	1.57	10.57	1.39	25.08	5.48
Cluster-36782.55910	Ribosomal RNA methyltransferase, putative [*Ixodes scapularis*]	2716	3.70E-176	22.24	5.17	7.52	0.36	11.78	8.31	7.73	4.88	16.63	10.11

SD standard deviation. FPKM values are the mean of the three biological replicates analyzed from each physiological condition and other information see Additional file 15: Table S9

Table 4 Partially *D. nuttalli* tick midgut heat shock proteins

Accession	Annotation	Gene length (bp)	*E* value	FPKM values Feeding time point									
				0 h	SD	24 h	SD	48 h	SD	72 h	SD	96 h	SD
Cluster-36782.55237	Heat shock factor-binding protein 1, partial [*Stegodyphus mimosarum*]	3058	6.10E-26	15.94	1.24	7.93	0.95	4.81	1.15	6.29	2.03	6.76	2.08
Cluster-36782.65311	Small heatshock protein I [*Rhipicephalus annulatus*]	1014	1.20E-66	342.59	54.48	2167.63	265.03	3759.40	637.18	2954.62	950.03	639.14	122.21
Cluster-36782.63871	Heat shock 70 kDa protein [*Haemaphysalis flava*]	2933	6.9e-311	330.07	51.07	117.28	10.83	284.36	45.73	230.81	1.36	200.76	34.15
Cluster-36782.79595	Heat shock HSP20 protein, putative [*Ixodes scapularis*]	4955	7.70E-63	1.94	0.51	25.13	2.56	9.66	3.46	9.09	1.55	6.61	1.04
Cluster-36782.45242	Heat shock protein 70 (HSP70)-interacting protein, putative [*Ixodes scapularis*]	1390	7.70E-77	8.51	1.02	20.26	1.71	9.53	2.80	14.79	6.55	6.55	2.00
Cluster-36782.88177	Heat shock protein 70–8804 [*Haemaphysalis flava*]	1325	5.90E-228	0.15	0.10	0.60	0.15	1.04	0.18	0.40	0.12	0.24	0.22
Cluster-36782.59911	Heat shock protein 90 [*Haemaphysalis flava*]	597	3.20E-24	9.06	0.99	2.68	1.84	2.04	1.74	1.14	0.51	1.75	1.74
Cluster-36782.74863	Heat shock protein HSP70-12A, putative, partial [*Ixodes scapularis*]	6968	2.30E-307	2.36	0.33	0.61	0.03	0.91	0.36	0.77	0.25	1.26	0.47

SD standard deviation. FPKM values are the mean of the three biological replicates analyzed from each physiological condition and other information see Additional file 16: Table S10

acquisition of Borrelia burgdorferi, yet in the midgut of female ticks, it had no such effect (Narasimhan et al. 2007). This discrepancy suggests that the same protein may fulfill distinct functions in different organs.

Conclusion

This study provides the first insights into *D. nuttalli* at the gene expression level from the first four days of blood feeding and discusses some important antigens that may participate in blood-feeding processes as well as multiple metabolic pathways such as nutrient absorption, energy production, and biosynthesis of essential molecules. These may provide a theoretical basis for the development of new strategies for the control of *D. nuttalli*. Moreover, this study identified the differentially expressed metabolic processes and cellular functions in the midgut of female *D. nuttalli* after feeding. Overall, these analyses provide a wealth of novel information that enhances our understanding of the biochemistry and physiology of blood digestion in the gut of *D. nuttalli*.

Supplementary Information The online version contains supplementary material available at https://doi.org/10.1007/s00436-025-08480-6.

Acknowledgements We thank all the research team members in our lab for their assistance. We also thank Novogene Bioinformatics Technology Co. (Beijing, China) for RNA-seq library construction and bioinformatics analysis through a service contract.

Author contribution All persons who meet authorship criteria are listed as authors, and all authors certify that they have participated sufficiently in the work to take public responsibility for the content, including participation in the concept, design, analysis, writing, or revision of the manuscript. Furthermore, each author certifies that this material or similar material has not been and will not be submitted to or published in any other publication before its appearance in the Parasitology Research. All authors contributed to the study conception and design. Material preparation, data collection and analysis were performed by HJM, LJJ and JF. HJM, CL, TSL contributed to get Dermacentor nuttalli. XNX and JXL designed the study. The first draft of the manuscript was written by YLS and all authors commented on previous versions of the manuscript. All authors read and approved the final manuscript.

Funding This study was supported by Chunhui Program of the Ministry of Education of the People's Republic of China (grant numbers 202201836), Qinghai University Research Ability Enhancement Project (2025KTST05), the Open Project of State Key Laboratory of Plateau Ecology and Agriculture, Qinghai University (grant numbers 2023-ZZ-13), and the Open Research Fund of Engineering Research Center of North-East Cold Region Beef Cattle Science & Technology Innovation.

Data availability The sequencing transcriptome data obtained were submitted to the National Center for Biotechnology Information Database (NCBI, accession number: PRJNA868620) in this study. Sequence Read Archive (SRA) has been deposited at NCBI under the accessions SRR21031626, SRR21031627, SRR21031628, SRR21031629, SRR21031630, SRR21031631, SRR21031632, SRR21031633, SRR21031634, SRR21031635, SRR21031636, SRR21031637, SRR21031638, SRR21031639, SRR21031640. Transcriptome Shotgun Assemblies (TSA) has been deposited at DDBJ/ EMBL/ GenBank under the accessions GKLF00000000.

Declarations

Ethical approval The experimental animals used in this project were treated in strict accordance with the Guidelines for Animal Ethics and Experimentation of the People' s Republic of China. The experimental animals were used in accordance with the protocols approved by The Scientifc Ethics Committee of Qinghai University (permit number: SL-2022007). The dead rabbits were uniformly cremated in the incinerator for the experimental animals at Qinghai University.

Consent to participate Not applicable.

Consent for publication Not applicable.

Competing interests The authors declare no competing interests.

References

Anderson JM, Sonenshine DE, Valenzuela JG (2008) Exploring the mialome of ticks: an annotated catalogue of midgut transcripts from the hard tick, *Dermacentor variabilis* (Acari: Ixodidae). BMC Genomics 20(9):552. https://doi.org/10.1186/1471-2164-9-552

Antunes S, Merino O, Mosqueda J, Moreno-Cid JA, Bell-Sakyi L, Fragkoudis R, Weisheit S, Pérez de la Lastra JM, Alberdi P, Domingos A, de la Fuente J (2014) Tick capillary feeding for the study of proteins involved in tick-pathogen interactions as potential antigens for the control of tick infestation and pathogen infection. Parasit Vectors 7:42. https://doi.org/10.1186/1756-3305-7-42

Aounallah H, Bensaoud C, M'ghirbi Y, Faria F, Chmelar JI, Kotsyfakis M (2020) Tick salivary compounds for targeted immunomodulatory therapy. Front Immunol 11:583845. https://doi.org/10.3389/fimmu.2020.583845

Bakdash JZ, Marusich LR (2017) Repeated measures correlation. Front Psychol 10:1201. https://doi.org/10.3389/fpsyg.2017.00456

Bendele KG, Guerrero FD, Cameron C, Bodine DM, Miller RJ (2019) Gene expression during the early stages of host perception and attachment in adult female *Rhipicephalus microplus*

ticks. Exp Appl Acarol 79(1):107–124. https://doi.org/10.1007/s10493-019-00420-1

Benoit JB, Lopez-Martinez G, Patrick KR, Phillips ZP, Krause TB, Denlinger DL (2011) Drinking a hot blood meal elicits a protective heat shock response in mosquitoes. Proc Natl Acad Sci USA 108(19):8026–9. https://doi.org/10.1073/pnas.1105195108

Das S, Banerjee G, DePonte K, Marcantonio N, Kantor FS, Fikrig E (2001) Salp25D, an *Ixodes scapularis* antioxidant, is 1 of 14 immunodominant antigens in engorged tick salivary glands. J Infect Dis 184(8):1056–64. https://doi.org/10.1086/323351

de la Fuente J (2012) Vaccines for vector control: exciting possibilities for the future. Vet J 194(2):139–40. https://doi.org/10.1016/j.tvjl.2012.07.029

Francischetti IM, Mather TN, Ribeiro JM (2003) Cloning of a salivary gland metalloprotease and characterization of gelatinase and fibrin(ogen)lytic activities in the saliva of the Lyme disease tick vector *Ixodes scapularis*. Biochem Biophys Res Commun. 305(4):869–75. https://doi.org/10.1016/s0006-291x(03)00857-x

Gettins PG (2002) Serpin structure, mechanism, and function. Chem Rev 102(12):4751–804. https://doi.org/10.1021/cr010170+

Gong H, Liao M, Zhou J, Hatta T, Huang P, Zhang G, Kanuka H, Nishikawa Y, Xuan X, Fujisaki K (2008) Gene silencing of ribosomal protein P0 is lethal to the tick *Haemaphysalis longicornis*. Vet Parasitol 151(2–4):268–78. https://doi.org/10.1016/j.vetpar.2007.11.015

Huntington JA (2006) Shape-shifting serpins–advantages of a mobile mechanism. Trends Biochem Sci 31(8):427–35. https://doi.org/10.1016/j.tibs.2006.06.005

Imamura S, da Silva Vaz Junior I, Sugino M, Ohashi K, Onuma M. (2005) A serine protease inhibitor (serpin) from *Haemaphysalis longicornis* as an anti-tick vaccine. Vaccine 23(10):1301-11.https://doi.org/10.1016/j.vaccine.2004.08.041

Jmel MA, Aounallah H, Bensaoud C, Mekki I, Chmelař J, Faria F, M'ghirbi Y, Kotsyfakis M, (2021) Insights into the role of tick salivary protease inhibitors during ectoparasite-host crosstalk. Int J Mol Sci 22(2):892. https://doi.org/10.3390/ijms22020892

Jongejan F, Uilenberg G (2004) The global importance of ticks. Parasitology 129(Suppl):S3-14. https://doi.org/10.1017/s0031182004005967

Kanehisa M (2019) Toward understanding the origin and evolution of cellular organisms. Protein Sci 28(11):1947–1951. https://doi.org/10.1002/pro.3715

Kanehisa M, Goto S (2000) KEGG: kyoto encyclopedia of genes and genomes. Nucleic Acids Res 28(1):27–30. https://doi.org/10.1093/nar/28.1.27

Kanehisa M, Furumichi M, Sato Y, Ishiguro-Watanabe M, Tanabe M (2021) KEGG: integrating viruses and cellular organisms. Nucleic Acids Res 49(D1):D545–D551. https://doi.org/10.1093/nar/gkaa970

Kocan KM, de la Fuente J, Blouin EF, Garcia-Garcia JC (2004) *Anaplasma* marginale (Rickettsiales: Anaplasmataceae): recent advances in defining host-pathogen adaptations of a tick-borne rickettsia. Parasitology 129(Suppl):S285-300. https://doi.org/10.1017/s0031182003004700

Langmead B, Salzberg SL (2012) Fast gapped-read alignment with Bowtie 2. Nat Methods 9(4):357–9. https://doi.org/10.1038/nmeth.1923

Lara FA, Pohl PC, Gandara AC, Ferreira Jda S, Nascimento-Silva MC, Bechara GH, Sorgine MH, Almeida IC, Vaz Ida S, Jr Oliveira PL, Jr (2015) ATP binding cassette transporter mediates both heme and pesticide detoxification in tick midgut cells. PLoS One 10(8):e0134779. https://doi.org/10.1371/journal.pone.0134779

Lee AW, Deruaz M, Lynch C, Davies G, Singh K, Alenazi Y, Eaton JRO, Kawamura A, Shaw J, Proudfoot AEI, Dias JM, Bhattacharya S (2019) A knottin scaffold directs the CXC-chemokine-binding specificity of tick evasins. J Biol Chem 294(29):11199–11212. https://doi.org/10.1074/jbc.RA119.008817

Li B, Dewey CN (2011) RSEM: accurate transcript quantification from RNA-Seq data with or without a reference genome. BMC Bioinformatics 4(12):323. https://doi.org/10.1186/1471-2105-12-323

Love MI, Huber W, Anders S (2014) Moderated estimation of fold change and dispersion for RNA-seq data with DESeq2. Genome Biol 15(12):550. https://doi.org/10.1186/s13059-014-0550-8

Lu S, Martins LA, Kotál J, Ribeiro JMC, Tirloni L (2023) A longitudinal transcriptomic analysis from unfed to post-engorgement midguts of adult female *Ixodes scapularis*. Sci Rep 13(1):11360. https://doi.org/10.1038/s41598-023-38207-5

Lu S, de Sousa-Paula LC, Ribeiro JMC, Tirloni L (2024) Exploring the longitudinal expression dynamics of midguts in adult female *Amblyomma americanum* ticks. BMC Genomics 25(1):996. https://doi.org/10.1186/s12864-024-10905-y

Ma H, Ai J, La Y, Zhao X, Zeng A, Qin Q, Feng S, Kang M, Sun Y, Li J (2023a) Hemalin vaccination modulates the host immune response and reproductive cycle of *Haemaphysalis longicornis*. Vet Parasitol 323:110051. https://doi.org/10.1016/j.vetpar.2023.110051

Ma H, Ai J, Kang M, Li J, Sun Y (2023b) The life cycle of *Dermacentor nuttalli* from the Qinghai-Tibetan Plateau under laboratory conditions and detection of spotted fever group *Rickettsia* spp. Front Vet Sci 10:1126266. https://doi.org/10.3389/fvets.2023.1126266

Mangia C, Vismarra A, Genchi M, Epis S, Bandi C, Grandi G, Bell-Sakyi L, Otranto D, Passeri B, Kramer L (2018) Exposure to amitraz, fipronil and permethrin affects cell viability and ABC transporter gene expression in an *Ixodes ricinus* cell line. Parasit Vectors 11(1):437. https://doi.org/10.1186/s13071-018-3020-4

Mate L, Ballent M, Cantón C, Lanusse C, Ceballos L, Alvarez LLI, Liron JP (2022) ABC-transporter gene expression in ivermectin-susceptible and resistant *Haemonchus contortus* isolates. Vet Parasitol 302:109647. https://doi.org/10.1016/j.vetpar.2022.109647

Mediannikov O, Matsumoto K, Samoylenko I, Drancourt M, Roux V, Rydkina E, Davoust B, Tarasevich I, Brouqui P, Fournier PE (2008) *Rickettsia raoultii* sp. nov., a spotted fever group rickettsia associated with *Dermacentor* ticks in Europe and Russia. Int J Syst Evol Microbiol 58(Pt 7):1635-9. https://doi.org/10.1099/ijs.0.64952-0

Miyoshi T, Tsuji N, Islam MK, Huang X, Motobu M, Alim MA, Fujisaki K (2007) Molecular and reverse genetic characterization of serine proteinase-induced hemolysis in the midgut of the ixodid tick *Haemaphysalis longicornis*. J Insect Physiol 53(2):195–203. https://doi.org/10.1016/j.jinsphys.2006.12.001

Miyoshi T, Tsuji N, Islam MK, Alim MA, Hatta T, Yamaji K, Anisuzzaman Fujisaki K (2010) A Kunitz-type proteinase inhibitor from the midgut of the ixodid tick, *Haemaphysalis longicornis*, and its endogenous target serine proteinase. Mol Biochem Parasitol 170(2):112–5. https://doi.org/10.1016/j.molbiopara.2009.12.005

Moraga-Fernández A, Muñoz-Hernández C, Sánchez-Sánchez M, Fernández de Mera IG, de la Fuente J (2023) Exploring the diversity of tick-borne pathogens: the case of bacteria (*Anaplasma*, *Rickettsia*, *Coxiella* and *Borrelia*) protozoa (*Babesia* and *Theileria*) and viruses (*Orthonairovirus*, tick-borne encephalitis virus and louping ill virus) in the European continent. Vet Microbiol 286:109892. https://doi.org/10.1016/j.vetmic.2023.109892

Mulenga A, Erikson K (2011) A snapshot of the *Ixodes scapularis* degradome. Gene 482(1–2):78–93. https://doi.org/10.1016/j.gene.2011.04.008

Mulenga A, Khumthong R, Chalaire KC (2009) *Ixodes scapularis* tick serine proteinase inhibitor (serpin) gene family; annotation and transcriptional analysis. BMC Genomics 10:217. https://doi.org/10.1186/1471-2164-10-217

Narasimhan S, Sukumaran B, Bozdogan U, Thomas V, Liang X, DePonte K, Marcantonio N, Koski RA, Anderson JF, Kantor F, Fikrig E (2007) A tick antioxidant facilitates the Lyme disease agent's successful migration from the mammalian host to the arthropod vector. Cell Host Microbe 2(1):7–18. https://doi.org/10.1016/j.chom.2007.06.001

Nathaly Wieser S, Schnittger L, Florin-Christensen M, Delbecq S, Schetters T (2019) Vaccination against babesiosis using recombinant GPI-anchored proteins. Int J Parasitol 49(2):175–181. https://doi.org/10.1016/j.ijpara.2018.12.002

Perner J, Provazník J, Schrenková J, Urbanová V, Ribeiro JM, Kopáček P (2016) RNA-seq analyses of the midgut from blood- and serum-fed *Ixodes ricinus* ticks. Sci Rep 8(6):36695. https://doi.org/10.1038/srep36695

Pohl PC, Klafke GM, Carvalho DD, Martins JR, Daffre S, da Silva Vaz I, Masuda A Jr (2011) ABC transporter efflux pumps: a defense mechanism against ivermectin in *Rhipicephalus* (*Boophilus*) *microplus*. Int J Parasitol 41(13–14):1323–33. https://doi.org/10.1016/j.ijpara.2011.08.004

Puente XS, Sánchez LM, Gutiérrez-Fernández A, Velasco G, López-Otín C (2005) A genomic view of the complexity of mammalian proteolytic systems. Biochem Soc Trans 33(Pt 2):331–4. https://doi.org/10.1042/BST0330331

Rahman MK, Kim B, You M (2020) Molecular cloning, expression and impact of ribosomal protein S-27 silencing in *Haemaphysalis longicornis* (Acari: Ixodidae). Exp Parasitol 209:107829. https://doi.org/10.1016/j.exppara.2019.107829

Rodríguez-Mallon A, Fernández E, Encinosa PE, Bello Y, Méndez-Pérez L, Ruiz LC, Pérez D, González M, Garay H, Reyes O, Méndez L, Estrada MP (2012) A novel tick antigen shows high vaccine efficacy against the dog tick, *Rhipicephalus sanguineus*. Vaccine 30(10):1782–9. https://doi.org/10.1016/j.vaccine.2012.01.011

Schlesinger MJ (1990) Heat shock proteins. J Biol Chem 265(21):12111–4

Schwarz A, Tenzer S, Hackenberg M, Erhart J, Gerhold-Ay A, Mazur J, Kuharev J, Ribeiro JM, Kotsyfakis M (2014) A systems level analysis reveals transcriptomic and proteomic complexity in *Ixodes ricinus* midgut and salivary glands during early attachment and feeding. Mol Cell Proteomics 13(10):2725–35. https://doi.org/10.1074/mcp.M114.039289

Shi J, Hu Z, Deng F, Shen S (2018) Tick-Borne Viruses. Virol Sin 33(1):21–43. https://doi.org/10.1007/s12250-018-0019-0

Silverman GA, Whisstock JC, Askew DJ, Pak SC, Luke CJ, Cataltepe S, Irving JA, Bird PI (2004) Human clade B serpins (ov-serpins) belong to a cohort of evolutionarily dispersed intracellular proteinase inhibitor clades that protect cells from promiscuous proteolysis. Cell Mol Life Sci 61(3):301–25. https://doi.org/10.1007/s00018-003-3240-3

Silverman GA, Bird PI, Carrell RW, Church FC, Coughlin PB, Gettins PG, Irving JA, Lomas DA, Luke CJ, Moyer RW, Pemberton PA, Remold-O'Donnell E, Salvesen GS, Travis J, Whisstock JC (2001) The serpins are an expanding superfamily of structurally similar but functionally diverse proteins. Evolution, mechanism of inhibition, novel functions, and a revised nomenclature. J Biol Chem 276(36):33293-6. https://doi.org/10.1074/jbc.R100016200

Simão FA, Waterhouse RM, Ioannidis P, Kriventseva EV, Zdobnov EM (2015) BUSCO: assessing genome assembly and annotation completeness with single-copy orthologs. Bioinformatics 31(19):3210–2. https://doi.org/10.1093/bioinformatics/btv351

Šimo L, Kazimirova M, Richardson J, Bonnet SI (2017) The essential role of tick salivary glands and saliva in tick feeding and pathogen transmission. Front Cell Infect Microbiol 7:281. https://doi.org/10.3389/fcimb.2017.00281

Sojka D, Franta Z, Horn M, Hajdusek O, Caffrey CR, Mares M, Kopácek P (2008) Profiling of proteolytic enzymes in the gut of the tick *Ixodes ricinus* reveals an evolutionarily conserved network of aspartic and cysteine peptidases. Parasit Vectors 1(1):7. https://doi.org/10.1186/1756-3305-1-7

Sonenshine DE, Macaluso KR (2017) Microbial invasion vs. tick immune regulation. Front Cell Infect Microbiol 7:390. https://doi.org/10.3389/fcimb.2017.00390

Song R, Ge T, Hu E, Fan X, Zhang Y, Zhai X, Li M, Zhang W, Wu L, Cheung AKL, Chahan B (2022) Recombinant cysteine proteinase as anti-tick targeting *Hyalomma asiaticum* infestation. Exp Parasitol 235:108234. https://doi.org/10.1016/j.exppara.2022.108234

Sun Y, He L, Yu L, Guo J, Nie Z, Liu Q (1897) Zhao J (2019) Cathepsin L-a novel cysteine protease from *Haemaphysalis flava* Neumann. Parasitol Res 118(5):1581–1592. https://doi.org/10.1007/s00436-019-06271-4

Tirloni L, Lu S, Calvo E, Sabadin G, Di Maggio LS, Suzuki M, Nardone G, da Silva Vaz I Jr, Ribeiro JMC (2020) Integrated analysis of sialotranscriptome and sialoproteome of the brown dog tick *Rhipicephalus sanguineus* (s.l.): insights into gene expression during blood feeding. J Proteomics 229:103899. https://doi.org/10.1016/j.jprot.2020.103899

Troxell B, Yang XF (2013) Metal-dependent gene regulation in the causative agent of Lyme disease. Front Cell Infect Microbiol 3:79. https://doi.org/10.3389/fcimb.2013.00079

Tutar L, Tutar Y (2010) Heat shock proteins; an overview. Curr Pharm Biotechnol 11(2):216–22. https://doi.org/10.2174/138920110790909632

Upadhyay AS, Vonderstein K, Pichlmair A, Stehling O, Bennett KL, Dobler G, Guo JT, Superti-Furga G, Lill R, Överby AK, Weber F (2014) Viperin is an iron-sulfur protein that inhibits genome synthesis of tick-borne encephalitis virus via radical SAM domain activity. Cell Microbiol 16(6):834–48. https://doi.org/10.1111/cmi.12241

van Zyl WA, Stutzer C, Olivier NA, Maritz-Olivier C (2014) Comparative microarray analyses of adult female midgut tissues from feeding *Rhipicephalus species*. Ticks Tick Borne Dis 6(1):84–90. https://doi.org/10.1016/j.ttbdis.2014.09.008

Villar M, Ayllón N, Busby AT, Galindo RC, Blouin EF, Kocan KM, Bonzón-Kulichenko E, Zivkovic Z, Almazán C, Torina A, Vázquez J, de la Fuente J (2010) Expression of heat shock and other stress response proteins in ticks and cultured tick cells in response to *Anaplasma* spp. Int J Proteomics 2010:657261. https://doi.org/10.1155/2010/657261

Wang Q, Pan YS, Jiang BG, Ye RZ, Chang QC, Shao HZ, Cui XM, Xu DL, Li LF, Wei W, Xia LY, Li J, Zhao L, Guo WB, Zhou YH, Jiang JF, Jia N, Cao WC (2021) Prevalence of multiple tick-borne pathogens in various tick vectors in Northeastern China. Vector Borne Zoonotic Dis 21(3):162–171. https://doi.org/10.1089/vbz.2020.2712

Webster A, Reck J, Santi L, Souza UA, Dall'Agnol B, Klafke GM, Beys-da-Silva WO, Martins JR, Schrank A (2015) Integrated control of an acaricide-resistant strain of the cattle tick *Rhipicephalus microplus* by applying Metarhizium anisopliae associated with cypermethrin and chlorpyriphos under field conditions.

Vet Parasitol 207(3-4):302-8. https://doi.org/10.1016/j.vetpar.2014.11.021.

Xavier MA, Tirloni L, Torquato R, Tanaka A, Pinto AFM, Diedrich JK, Yates JR 3rd, da Silva Vaz I, Seixas A Jr, Termignoni C (2019) Blood anticlotting activity of a *Rhipicephalus microplus* cathepsin L-like enzyme. Biochimie 163:12–20. https://doi.org/10.1016/j.biochi.2019.04.025

Xu X, Chang BW, Mans BJ, Ribeiro JM, Andersen JF (2013) Structure and ligand-binding properties of the biogenic amine-binding protein from the saliva of a blood-feeding insect vector of Trypanosoma cruzi. Acta Crystallogr D Biol Crystallogr 69(Pt 1):105–13. https://doi.org/10.1107/S0907444912043326

Xu XL, Cheng TY, Yang H, Liao ZH (2015) De novo assembly and analysis of midgut transcriptome of *Haemaphysalis flava* and identification of genes involved in blood digestion, feeding and defending from pathogens. Infect Genet Evol 38:62–72. https://doi.org/10.1016/j.meegid.2015.12.005

Zhang YK, Zhang XY, Liu JZ (2019) Ticks (Acari: Ixodoidea) in China: geographical distribution, host diversity, and specificity. Arch Insect Biochem Physiol 102(3):e21544. https://doi.org/10.1002/arch.21544

Zhao GP, Wang YX, Fan ZW, Ji Y, Liu MJ, Zhang WH, Li XL, Zhou SX, Li H, Liang S, Liu W, Yang Y, Fang LQ (2021) Mapping ticks and tick-borne pathogens in China. Nat Commun 12(1):1075. https://doi.org/10.1038/s41467-021-21375-1